Bonding-Geometry Dependence of Fractal Growth on Metal Surfaces

Zhenyu Zhang, Xun Chen, and Max G. Lagally
University of Wisconsin, Madison, Wisconsin 53706
(Received 22 March 1994)

Mechanisms for the formation of two-dimensional fractal shapes in metal-on-metal growth have been investigated theoretically. It is shown that an extended fractal growth regime, characterized by significant local edge diffusion, exists on triangular but not on square lattices. Simulations to fit observed data allow estimates of the activation barrier for edge diffusion.

PACS numbers: 68.35.Bs, 68.55.Jk, 68.70.+w, 82.20.Mj

Recent scanning tunneling microscopy (STM) studies of metal-on-metal growth at submonolayer coverages have uncovered a striking phenomenon. Within comparable ranges of growth conditions, fractal-like islands have frequently been observed on substrates of triangular or hexagonal geometry [1–3], but to date only compact islands have been observed on substrates with square geometry [4–6]. The only exception is the heteroepitaxial growth of Ag on Ni(100) [7], for which dendritic step decoration has been observed on a square lattice, but where the adatoms themselves again assume a triangular geometry.

The underlying physical reason for the dependence of the submonolayer growth laws on the *substrate* or *growth* geometry has so far not been explored. The observed fractal structures have traditionally been attributed to diffusion limited aggregation (DLA) [8]. Theoretical studies addressing STM observations of fractal growth have neglected the difference in substrate geometry, using instead square lattices in growth simulations [9–13]. But in the standard hit-and-stick DLA model, fractal growth should take place on both square and triangular lattices [8,14]. In addition, a morphological difference between the observed [1,2] and the standard DLA fractal structures is apparent to the naked eye. In the STM images, the average arm thickness of the fractal islands is about four or more atoms [1,2], while in the DLA model this thickness is only one atom. Widening of the arm thickness can be expected if the atom-island sticking coefficient is less than 1 [14–16]. But a reduced atom-island sticking coefficient cannot be the cause at the conditions at which fractal structures are observed because lateral evaporation of atoms from islands is negligible.

In this Letter, we study theoretically metal-on-metal growth at submonolayer coverages on both a triangular and a square lattice, using realistic growth models and physical parameters. We pay special attention to the specific atomic-bonding geometries in the two cases. We show that under otherwise identical growth conditions, the difference between the local atomic-bonding configurations gives rise to the fundamentally different growth laws on the two lattices. In particular, the temperature range for fractal growth is predicted to be much wider on a triangular lattice than on a square lattice. Furthermore, our results suggest that the formation of essentially all the observed fractal structures in recent experimental studies [1,2] has involved significant local relaxation via edge diffusion. These fractals are distinctly different from those formed within the standard DLA model.

We begin with a qualitative analysis, followed by a semiquantitative dimensional analysis, and finally by a presentation of results of kinetic Monte Carlo simulations. Qualitatively, at very low temperatures the DLA model is valid for all lattices [8,14,15]. The temperature range defining this regime will be discussed below. As the substrate temperature is increased with all other growth parameters kept constant, an atom previously inhibited from moving by only one in-plane nearest neighbor (nn) will become mobile along the edge of the island. For a square lattice, the atom remains edge mobile until it finds a more stable kink site, where it has multiple nearest neighbors [Fig. 1(a)]. The resulting growth morphology is compact. In contrast, for a triangular lattice, this edge diffusion can only be local, because the atom will easily find a site with two nearest neighbors [Fig. 1(b)], and further diffusion away from a twofold coordinated site would require higher thermal energy. The switching of the *inhibition* mechanism from 1–nn binding to 2–nn binding preserves the fractal growth mode, because there are still a large number of *degenerate* sites at which

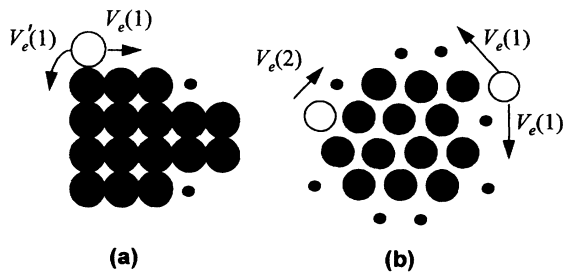

FIG. 1. (a) Stable sites on a square; (b) triangular lattice once a onefold coordinated atom (open circle) bound to the island edge becomes mobile. The stable sites are marked by the small circles. Possible activation barriers for diffusion by the edge atoms are shown.

growth can proceed. Fractal growth will be replaced by compact growth only at temperatures at which even inhibition by 2–nn binding becomes ineffective.

The above qualitative analysis offers a possible explanation why fractal growth is observed only on triangular lattices: For square lattices, the transition from the standard DLA regime (hereafter called regime I) to the compact growth regime (regime III) is direct. But for triangular lattices, an *extended* fractal growth regime (regime II) is sandwiched in between (see Fig. 2).

Using dimensional analysis, we can further assess the temperature dependence of the crossover processes from one growth regime to another. For submonolayer coverage, the growth morphology is mainly determined by the interplay between the deposition rate, k_r, the hopping rate for single-atom diffusion, k_s, and the rate for edge diffusion, k_e. All other rate processes are either too slow (such as the evaporation of an adatom from an island) or unimportant (such as the rate controlling interlayer particle transport). The neglect of adatom evaporation is equivalent to saying that the critical island size is 1 [17]. The island density is determined by the first two rates: a high density of small islands for k_s/k_r small, and a low density of large islands for k_s/k_r large. The *compactness* of the islands is determined by *all* the three rates. When k_s/k_r is very small, it is not meaningful to talk about the fractal dimensionality of the islands, because they are too small. When this ratio is large enough such that the islands are large and well separated from each other, then the value of k_e determines whether they possess fractal structures. A necessary condition to allow fractal structures in regime I is $k_e(1)/k_s < 1$, where $k_e(1)$ is the edge diffusion rate from a *onefold* coordinated site. Here we introduce p to be the number of hops an atom bound to the edge of an island will make along the edge before being joined by a second atom arriving from the 2D vapor created by the deposited atoms. Then $p = k_e t_1$, where t_1 is the time separation between two consecutive arrivals at the same edge site. This time is given by

$$t_1 = O(1)\left\{\frac{\theta^{d+2}}{R^{2d+1}D^{d-1}}\right\}^{1/3d}. \quad (1)$$

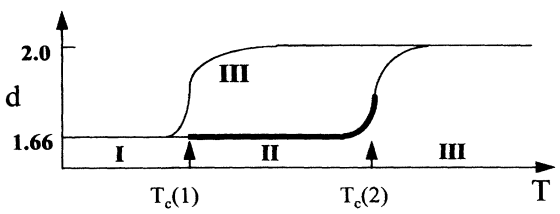

FIG. 2. "Phase" diagram showing three possible growth regimes: (I) standard DLA; (II) extended fractal; (III) compact. Regime II exists only for triangular lattices, as marked by the thicker segment of the lower curve. d is the fractal dimension.

Here R is the deposition rate, θ the coverage, $D = a^2 k_s$ the single-atom diffusion coefficient, a the hopping distance, and d the (fractal) dimensionality of the islands. In deriving Eq. (1), we have assumed two-dimensional isotropic diffusion, and have invoked the relation that the number of edge sites along a fractal island of size N is given by $N_e \approx 2\pi(N/\pi)^{1/d}$. The rest of the derivation follows standard incorporation and nucleation theory at low coverages [18]. Expressing $k_i = \nu_i \exp\{-\beta V_i\}$, with $\nu_i = \nu_e$ or ν_s the attempt frequency for edge or terrace diffusion, $V_i = V_e$ or V_s the corresponding activation barrier, and $\beta = 1/kT$, we have

$$p = O(1)\,\nu_e \left\{\frac{\theta^{d+2}}{(a^2\nu_s)^{d-1}R^{2d+1}}\right\}^{1/3d} \times \exp\left\{-\frac{1}{kT}\left(V_e - \frac{d-1}{3d}V_s\right)\right\}. \quad (2)$$

Equation (2) shows how the value of p, which controls the compactness of the islands, depends on external (R, T, and θ) and internal (ν_e, ν_s, V_e, and V_s) physical parameters. In subsequent discussions we assume $\nu_e = \nu_s$.

If $V_e(1) < V_s$, where $V_e(1)$ is the barrier for diffusion along the edge of an island by an atom bound to the island by only one nn bond, the DLA regime is unreachable.

For systems that do satisfy $V_e(1) > V_s$ (i.e., edge diffusion is slower than terrace diffusion), we can draw a "phase" diagram using Eq. (2) (see Fig. 2). At very low temperatures, $p \ll 1$ and we have fractal growth by DLA, with a fractal dimension $d = 1.66$. This behavior occurs for all types of lattices [8,14,15]. As T is raised, the probability p that an atom bound to the edge makes a hop increases exponentially, quickly reaching the crossover region $p \sim 1$. For a square lattice, the activation barrier against edge diffusion consists of the breaking and the rejoining of one nn bond. The shape of the islands quickly changes from being fractal to being compact as the value of p increases from $p \ll 1$ to $p \gg 1$. The corresponding dimensionality of the islands changes from 1.66 to 2 [12,13]. The transition temperature, located near the center of the crossover region, is given by

$$T_c(1) = \frac{1}{k}\left\{V_e(1) - \frac{d-1}{3d}V_s\right\} \times \ln^{-1}\left\{\nu_e\left[\frac{\theta^{d+2}}{(a^2\nu_s)^{d-1}R^{2d+1}}\right]^{1/3d}\right\}. \quad (3)$$

For triangular lattices, when inhibition by 1-nn binding fails to prevent an atom from hopping along the edge, inhibition by 2-nn binding occurs, as the atom increases its coordination number by one after making a limited number of hops. This amounts to replacing $V_e(1)$ in

Eq. (2) by $V_e(2)$ [see Fig. 1(b)]. Fractal growth takes place as long as $V_e(2)$ is effective in preventing an edge atom from leaving a twofold coordinated site in the time it takes for another atom to arrive. The temperature range defining this regime II in fractal growth is given by $k\Delta T = [V_e(2) - V_e(1)]\ln^{-1}(A)$, where A is the argument of the logarithm in Eq. (3). Figure 2 contrasts schematically the behavior for the two lattices, assuming identical growth conditions and effective bond strengths. The crossover from fractal to compact at either $T_c(1)$ or $T_c(2)$ is exponentially fast.

For the triangular lattice, we have chosen the same fractal dimension in regimes I and II, implying that the two regimes belong to the same universality class. This conclusion is reached from computer simulations using the following minimal model. First, we repeat the simulation for the DLA model [8]. A typical island in this regime I is shown in Fig. 3(a). Next we simulate the case where the temperature is halfway between $T_c(1)$ and $T_c(2)$, such that every atom reaching the island will make hops until it is at least twofold coordinated. A typical island in this case is shown in Fig. 3(b), which looks distinctly different from Fig. 3(a), but a standard analysis yields the same fractal dimension $d = 1.66$. What differentiates them is the shape factor, S, defined by $N = Sr^d$, where N is the number of atoms contained within an island of radius of gyration r. In regime I, $S = 4.2$, while in regime II, $S = 7.6$. We can also introduce a physically more transparent measure for differentiating the two regimes, the coordination number distribution plotted in Fig. 4. In regime I, this distribution is peaked at 2, as expected; the corresponding average thickness of the arms of the island is about 1. In regime II, the peaked value is shifted up to 5, with an average arm thickness approximately equal to 4. We stress that these results hold as long as the difference between $V_e(1)$ and $V_e(2)$ is sizable, making the center of regime II well defined; they do not depend on the precise value of either $V_e(1)$ or $V_e(2)$.

We now return to the question why fractal 2D growth structures have been observed experimentally only on triangular lattices. First, why are they *not* observed on square lattices? On square lattices it is only possible to grow fractals in regime I. The absence of fractals on square lattices could be due simply to the trivial fact that $V_e(1) < V_s$ for all the square-lattice systems that have been investigated; this is equivalent to saying that $T_c(1) \sim 0$. Simple bond counting and calculation using density functional theory suggest $V_e(1) > V_s$ [19]. Standard solid-on-solid growth simulations on square lattices typically also assume this inequality [12,13,20]. But as long as $V_e(1)$ is not considerably higher than V_s, growth at very low temperatures with extremely low deposition rate is required in order to observe the possible formation of islands with fractal shapes. The chance of observing fractal growth on square lattices is expected to be higher on substrates where enhanced terrace diffusion by concerted atomic motion can take place [21].

For triangular lattices, it is possible to reach both fractal growth regimes I and II if $V_e(1) > V_s$. Even if $V_e(1) < V_s$, but as long as $V_e(2) > V_s$, regime II, defined now between 0 K and $T_c(2)$, is still achievable. In fact, based on the arm thickness of the fractal islands shown in the STM images [1,2], we conclude that all these fractals have been formed in regime II.

We can make some useful upper-bound estimates on $V_e(1)$ for several systems. For Fe/Fe(100), compact island growth was observed at 20 °C, the lowest temperature explored [4]. Using Eq. (3) with $d = 2$, and experimental values $\theta = 0.07$ ML (monolayer), $R = 1.4 \times 10^{13}$ atoms $\mathrm{cm}^{-2}\,\mathrm{s}^{-1}$, $V_s = 0.45$ eV, $D_0 = a^2\nu_s = 7.2 \times 10^{-4}$ $\mathrm{cm}^2\,\mathrm{s}^{-1}$, and also assuming $\nu_e \approx \nu_s$, we get an *upper-bound* estimate of $V_e(1)$ to be 0.65 eV.

For Pt/Pt(111), fractal growth was observed at 200 K [2]. First, in order to estimate V_s we have done growth simulations on a triangular lattice at experimentally defined conditions [see Fig. 5(a)], and compared the island density with the STM experiments [2]. The resulting V_s is 0.25 eV, which agrees well with the value from field ion microscope (FIM) measurements [22] and lies between theoretical predictions [22,23]. No experimental or reliable theoretical information is available about $V_e(1)$. Because the fractal structures observed by STM resemble the simulated fractal structures in regime II, $T_c(1)$ must be

(a) (b)

FIG. 3. Typical fractal islands formed on a triangular lattice, in (a), regime I, and (b), regime II.

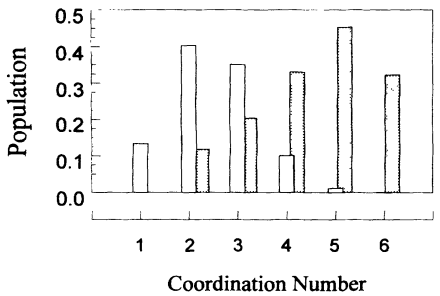

FIG. 4. Coordination number distribution for the fractal islands shown in Figs. 3(a) (open bars) and 3(b) (shaded bars).

(a) (b)

FIG. 5. Islands grown on a (a) triangular and a (b) square lattice, at identical conditions. The lattice size is 200×200 in each case, and periodic boundary conditions have been imposed.

lower than 200 K at the growth conditions of the experiments. Using again Eq. (3) and setting $T_c(1) = 200$ K, we can give an *upper-bound* estimate of $V_e(1)$ for Pt/Pt(111) of 0.4 eV. An early FIM measurement [24] of V_e giving 0.5 eV at high temperature is presumably $V_e(2)$.

Finally we compare growth simulation results on different lattices using identical growth parameters: $T = 200$ K, $\theta = 0.2$ ML, $R = 0.01$ ML/s, $V_s = 0.25$ eV, $V_e(1) = 0.35$ eV, $V_e'(1) = 0.45$ eV, $V_e(2) = 0.5$ eV, and $\nu_0 = \nu_e = 8 \times 10^{12}$ s^{-1}. These parameters were chosen from the conditions at which fractal islands have been observed for Pt/Pt(111) [2]. The islands formed on a triangular lattice are shown in Fig. 5(a). They resemble the STM images closely [2]. The islands formed on a square lattice [Fig. 5(b)] are much more compact. Not shown here are results from separate simulations on a square lattice, using parameters as specified above for Fe/Fe(100) [4]. The resulting islands are small and compact, as observed in the experiments [4].

In conclusion, we have shown that it is critically important to take specific atomic-bonding geometry into proper consideration in modeling fractal growth on metal surfaces. An extended fractal growth regime may exist on triangular lattices, but is absent on square lattices. We have defined the transition temperatures bracketing this regime, using both external and internal physical parameters. We have also characterized the morphological differences between the fractal islands formed in this regime, and those formed using the standard DLA model. Our results suggest that essentially all the fractal structures observed in recent STM growth studies are formed in this extended regime.

We thank A. Zangwill, M. Bott, and C. Teichert for useful discussions, and J. Wu and P. Yang for assistance. This work was supported by NSF, MRG Grant No. DMR91–21074, and by NSF, Solid State Chemistry Grant No. DMR93–04912.

[1] R. Q. Hwang, J. Schroder, C. Gunther, and R. J. Behm, Phys. Rev. Lett. **67**, 3279 (1991); R. Q. Hwang and R. J. Behm, J. Vac. Sci. Technol. B **10**, 256 (1992).
[2] T. Michely, M. Hohage, M. Bott, and G. Comsa, Phys. Rev. Lett. **70**, 3943 (1993); M. Bott, T. Michely, and G. Comsa, Surf. Sci. **272**, 256 (1992).
[3] D. D. Chambliss and R. J. Wilson, J. Vac. Sci. Technol. B **9**, 928 (1991).
[4] J. A. Stroscio, D. T. Pierce, and R. A. Dragoset, Phys. Rev. Lett. **70**, 3615 (1993).
[5] E. Kopatzki, S. Gunther, W. Nichtl-Pecher, and R. J. Behm, Surf. Sci. **284**, 154 (1993).
[6] H. J. Ernst, F. Fabre, and J. Lapujoulade, Phys. Rev. B **46**, 1929 (1992).
[7] A. Brodde, G. Wilhelmi, D. Badt, H. Wengelnik, and H. Neddermeyer, J. Vac. Sci. Technol. B **9**, 920 (1991).
[8] T. A. Witten and L. M. Sander, Phys. Rev. Lett. **47**, 1400 (1981).
[9] T. Nagatani, J. Phys. Soc. Jpn. **62**, 981 (1993).
[10] L.-H. Tang, J. Phys. I (France) **3**, 935 (1993).
[11] J. G. Amar, F. Family, and P.-M. Lam, (to be published).
[12] G. S. Bales and D. C. Chrzan (to be published).
[13] C. Ratsch, A. Zangwill, P. Smilauer, and D. D. Vvedensky, Phys. Rev. Lett. **72**, 3194 (1992).
[14] T. A. Witten and L. M. Sander, Phys. Rev. B **27**, 5686 (1983).
[15] P. Meakin, Phys. Rev. A **27**, 1495 (1983).
[16] T. Vicsek, Phys. Rev. Lett. **53**, 2281 (1984).
[17] M. C. Bartelt and J. W. Evans, Phys. Rev. B **46**, 12675 (1992).
[18] J. A. Venables, Philos. Mag. **27**, 697 (1973); Y. W. Mo, J. Kleiner, M. B. Webb, and M. G. Lagally, Surf. Sci. **268**, 275 (1992); A. Pimpinelli, J. Villian, and D. E. Wolf, Phys. Rev. Lett. **69**, 985 (1992).
[19] R. Stumpf and M. Scheffler, Phys. Rev. Lett. **72**, 254 (1994).
[20] P. Smilauer, M. R. Wilby, and D. D. Vvedensky, Phys. Rev. B **47**, 4119 (1993).
[21] See a recent review by P. J. Feibelman, in Comments Condens. Matter Phys. **16**, 191 (1993), and references therein.
[22] P. J. Feibelman, J. S. Nelson, and G. L. Kellogg, Phys. Rev. B **49**, 10548 (1994).
[23] S. D. Liu, Z. Y. Zhang, G. Comsa, and H. Metiu, Phys. Rev. Lett. **71**, 2967 (1993).
[24] D. W. Basset and P. R. Webber, Surf. Sci. **70**, 520 (1978).

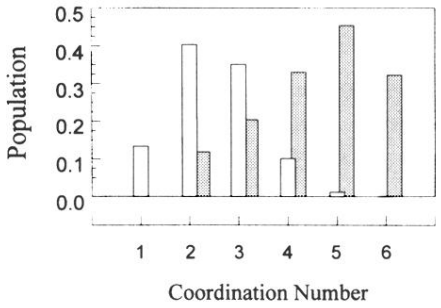

FIG. 4. Coordination number distribution for the fractal islands shown in Figs. 3(a) (open bars) and 3(b) (shaded bars).